A REPORT ON

Modeling of Organic Semiconductors

June 4, 2010

Submitted By:

JAYANT P. THATTE[1]

Mentor:

PROF. K. S. NARAYAN[2]

Jawaharlal Nehru Centre for Advanced Scientific Research, Jakkur

Bengaluru 560 064, India

Abstract

The report starts with the basics of how charge diffusion takes place through organic solids, giving a brief overview about behavior of intercalating ions in a thin film, trap states and its equivalent RC circuits. With this background, the next sections talk about two applications of organic semiconductors. The major application beingsolar cells. Sections 4 and 5 deal with solar cells, conventional model, need for a different model for organic solar cells and describes the new models which can be used to simulate organic solar cells in DC and AC simulations respectively. Extraction of physical parameters of a solar cell from its I-V curve by two different methods is discussed in sections 6 along with the discussions about accuracy of the two methods. Section 7 and 8 deal with basic theory of Electrolyte Polymer Interface (EPI) and its equivalent circuit. Based on this knowledge, the last section deals with modelling of human nerves with an equivalent circuit and finding equivalent circuit in particular for the retinal neurons involved in retinal electrography.

[1]Department of Electrical Engineering, Indian Institute Of Technology Madras, Chennai. Phone : 09962266524; email : meetjayant@gmail.com

[2]Head of Molecular Electronics Laboratory, Jawaharlal Nehru Centre for Advanced Scientific Research, Bengaluru. email : narayan@jncasr.ac.in

1 Introduction

Silicon has been celebrated for years as the most popular element in the semiconductor industry. All semiconductor devices are made of a semiconductor material, a conductor and an insulator. Semiconductor is amorphous silicon, conductor is doped silicon and insulator in silicon oxide. Thus, silicon is probably the only element to display all three properties under different forms. Moreover, interconversion between silicon and its oxide is very easy industrially. This is one of the main reasons for the widespread use of silicon in the semiconductor industry.
Silicon, however, has a drawback. If the dimensions of the component are large (e. g. solar panels, television screens etc.) then manufacturing a single wafer of pure silicon becomes very difficult and costly. This is where organic semiconductors (OS) come into picture. Fabrication of OS is extremely simple. The OS material is converted to ink and then any required circuit can be simply printed out. Solar energy tapping is one of the most essential tasks before mankind in the view of energy crisis. Bulk Heterojunction Polymer Solar Cells are promising candidates for economic solution for renewable energy source with relatively low manufacturing complexity. The OS are thus gaining an increasing importance.
The physics behind OS and their working is not understood as completely as that for inorganic semiconductors. It is therefore necesssary to understand the physics behind semiconductors in order to be able to build a model for OS. The next section deals with the basics of OS and how charge transfer takes place in OS.

2 General OS Theory : Trapped States and Ion Diffusion in Organic Semiconducting Material

2.1 Introduction

It is well established that ion motion in a solid environment occurs by hopping between localized sites. Ions reside for most of the time at minimum energy sites, but eventually they jump from one site to another overcoming the intersite barrier by a thermally activated process. Such sites are calles intercalation sites. There are different types of intercalation sites: a set of connected shallow sites which allow fast diffusion of the intercalating ions throughout the material, and slower types of sites which trap the intercalating ions.

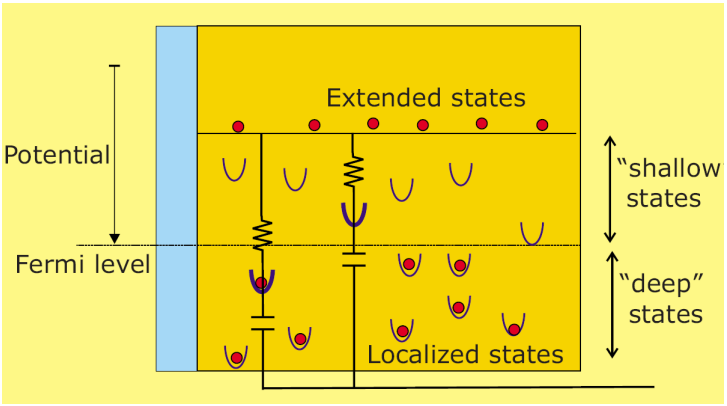

Semiconductors have both extended states (e. g. conduction band levels) and localised levels. The Fermi level approximately separates the occupied and the empty levels. Each trap state in a semiconductor is equivalent to an RC circuit. The equivalent circuits for two specific levels are shown in the above diagram. For each level, the resistance corresponds to the thermal release of the ions to the extended states. Thus, the resistance of the equivalent RC circuit depends upon the energy or potential difference between the trap level and the extended states and also the occupancy of the trap state. This resistance is called extraction resistance. The capacitance refers to the energy stored in the trapped state and hence depends upon both the energy of the trap state above the localised levels and the occupancy of the trap state. This capacitance is a new type of capacitance called Chemical Capacitance [1-2] also known as Accumulation Capacitance [3]. The extended levels also posses chemical capacitance although it is not shown in the diagram.

2.2 Fast state capacitance

The intercalating ions fill the fast states uniformly. This charging and discharging of the fast sites with ions according to the externally applied voltage can be discribed in terms of a capacitance called Fast State Capacitance and is denoted by C_0.

2.3 Ion Trapping Process

The slower types of sites are difficult to access and do not get filled immediately like the fast sites. These sites can get filled provided we wait for sufficient time.

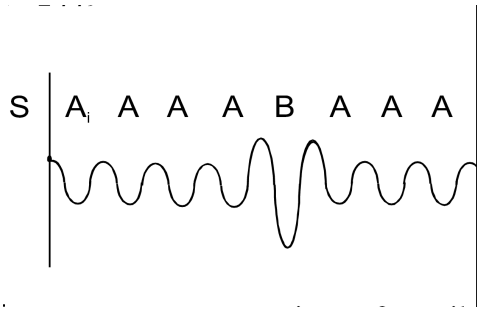

The fast states network consists of a region connected by relatively low barriers, and the hopping of these, i.e. the transitions A→A in Fig. 1, determines a diffusion coefficient for the fast charging mode. The system contains in addition single sites B or domains isolated by larger energy barriers, requiring a much longer time for its overcoming A→B. Hence, a fraction of the intercalated ions have been immobilized at certain sites, and do not participate in diffusion. Hence, for the equilibrium (low frequency) intercalation capacitance being larger than the diffusion capacitance. Trapping arises from the fact that mobile ions occupy different types of sites in the lattice. Sites separated by the larger energy barriers involve larger hopping times, and sites deep in energy involve large release times. In this sense trapping depends upon the time of residence of ions in a particular site.

2.4 Trapped Charge Capacitance

The total charge passed to the host solid increases as the time passes. This is because the connected sites AAA... (see above figure) get filled fast and the sites surrounded by large energy barriers go on filling slowly as the time passes. Hence the net capacitance due to the charging host is not limited to the fast state capacitance C_0but also has contribution from each of the trap states.

$$C_{total} = C_0 + C_{trap} \tag{1}$$

2.5 Model for Charging of Thin Film

A charging thin film can be modeled as shown below.

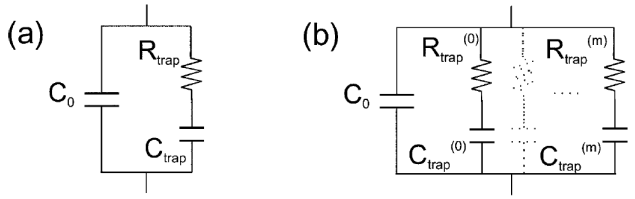

Figure (a) shows the single trap model while figure (b) shows multiplt trap model.

3 Applications

After knowing the basic theory about OS, one can move on to its applications. OS material is used widely for

- Photovoltaic Cells : These cells are used for tapping solar energy and also as detectors.
- OS Electrolyte Interface (Electrolyte Polymer Interface): This is used mostly in chemical batteries, solar cells etc.

Let us consider these two major applications in detail. Sections 4 to 7 deal with Organic Solar Cells and Electrolye Polymer Interface (EPI).

4 Model for Organic Solar Cells (OSC)

4.1 Difference Between OSC and Silicon-Based Solar Cells

Currently, OSC have a much lower efficiency as compared to that of the conventional thin film amorphous silicon solar cells (SSC) which is $\sim 10\%$. This difference arises due to different fundamental mechanism of current generation in the two types of cells. In SSC, onfalling light causes the generation of electron-hole pairs (EHP) which recombine through the external circuit giving rise to current. In most organic solar cells, however, the incident light only causes excitations and not EHP because the electron binding energy is high. A simple OSC consists of donor and acceptor layers of OS. The excitations produced in the donor diffuse to the donor-acceptor (D/A) interface and dissociate to form polaron pairs. These polarons can either recombine or dissociate into free charge carriers[3]. These dissociations are mainly driven by the strong electric field present in the space charge region of the D/A interface. (More details in section 7).

The reason for low efficiency is that the minimum thickness of the donor layer needed for efficient light absorption is considerably more than the maximum thickness upto which the photoexcitations can diffuse. This means that only a fraction of the excitations is actually converted to current. Again, depending upon the mobility of the electrons and holes, some of the EHP recombine within the OS layer iteslf and only the remaining are obtained as current output. This leads to quite low efficiency for OSC of $\sim 2-3\%$.

To overcome this problem, bulk heterojunctions consisting of an interpenetrating network of donor and acceptor materials have been used to ensure that all photo-generated excitons find a D/A interface within a diffusion length.

[3]Organic solar cells convert excitations into separated electrons and holes primarily at the D/A interfaces because the organic semiconductors on which the cells are based are excitonic in nature. The excitonic nature causes electron and hole pairs that form by absorption of light to be bound together by several tenths of an electron volt, a binding energy that is much greater than ambient thermal energy. At the D/A interfaces, the driving force to separate the charge carriers is great enough to overcome this binding energy.

Bulk heterojunctions have increased the efficiency of organic photovoltaic cells to 3-4% [4].

4.2 Existing Model for Solar Cells

All existing models of solar cells assume that the current by the cell is constant for a given light intensity. The conventional model of solar cell is shown in the following two figures.

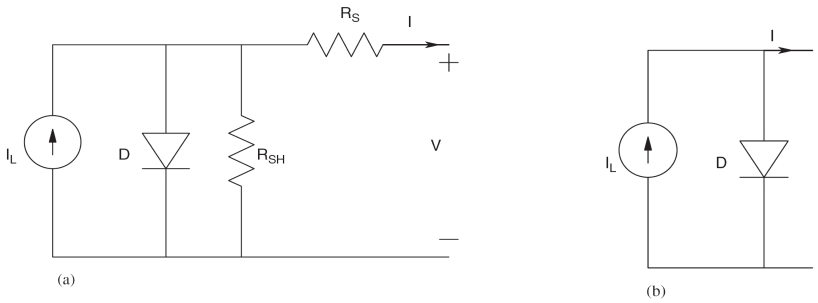

The first figure shows model with parasitic resistances $R_S$andR_{Sh}. The second one is the ideal version without these resistances. Let $I_L$be the generated current. Let the I-V characteristics of the cell be denoted as $I = f(V)$. This maximum current is called I_{SC}. The open circuit voltage of the cell is called V_{OC}. Then the measued current of the cell can be expressed as:

$$I = I_L - f(V) \tag{2}$$

As one can observe,

$$f(V_{OC}) = I_L \tag{3}$$

4.3 New Model for OSC and its Need

All the existing models for SSC assume that the current generated is constant for a given light intensity. Although this assumption holds good for inorganic solar cells, it does not hold for their organic counterparts. How effectively the excitations diffuse to the D/A interface also depends upon the electric field present inside the cell, which in turn depends on the voltage applied across its terminals. The current provided by the cell reduces when voltage applied across its terminals increases. Thus the current is maximum when the output terminals of cell are shorted.

A more appropriate assumption for OSC is that the generation rate of polaron pairs is constant for a given light intensity. Some of these may recombine internally. Thus the following change can be made in the conventional model to get an appropriate model for the OSC.

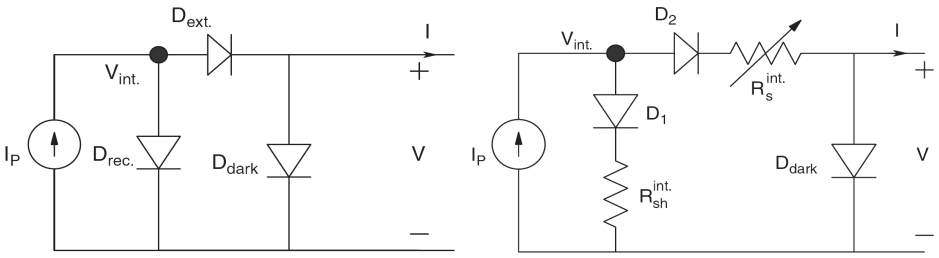

In the above model, $I_P$represents the total polaron pair generation rate. The diode D_{rec}represents the loss in output current due to internal recombination of the polaron pairs, diode D_{ext}represents the extraction of the dissociated free carriers and diode D_{dark}represents the I-V chracteristics of the cell under dark conditions. Note that while taking I-V characteristics in dark, D_{ext}becomes reverse biased and therefore only D_{dark}contributes to the I-V characteristics. $D_{rec}$and D_{ext}have an effect only under light conditions. We can write

$$I = I_P - I_{rec} - f(V) \tag{4}$$

$$I_{rec} = f_{rec}(V_{int}) \tag{5}$$

where f_{rec}represents the I-V characteristic of D_{rec}. $I_{SC}$is given by the following two expressions

$$I_{SC} = I_P - f_{rec}(V_{int}) \tag{6}$$

$$I_{SC} = f_{ext}(V_{int}) \tag{7}$$

One can notice that as the applied voltage is in reversed bias with respect to D_{ext}, the current flowing across it, under light conditions, will reduce until finally when the applied voltage is sufficient to make the current zero. This is V_{OC}.

A parameter $\xi$is used to express the departure of the OSC from conventional inorganic cells.

$$\xi = f(V_{OC})/I_{SC} \tag{8}$$

For inorganic cells, current remains constant, and hence for an ideal inorganic cell, $\xi = 1$. Whereas in the other extreme case $f(V_{OC}) = 0$and hence $\xi = 0$. Thus for a cell under consideration, if $\xi$is close to unity, then the conventional model for solar cells can be used. However, if the departure of ξ from unity is significant, then this new model would prove to be more accurate.

4.4 Changes in Model for AC simulations

The model given above is used onlt to obtain the DC characteristics of solar cells. For AC characteristcs, the model will have to be modified. Firstly, since the cell is made up of OS, instead of having only a shunt resistance R_{sh}, we will

now also have the fast state capacitance and the trap capacitance in series with extraction resistance (Refer section 2). Also, the diodes are used only in the DC Model. Hence, the solar cell model that should be used for AC is shown below.

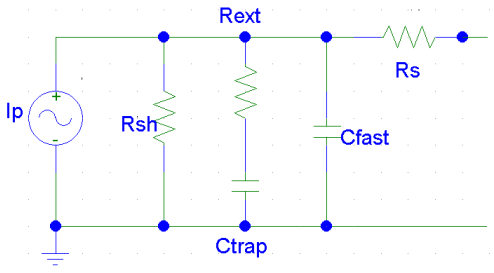

Note that all the above resistance and capacitance values depend upon the surface area of the solar cell and hence are usually expressed as Ωcm^2 and F/cm^2. Current is also expressed as mA/cm^2.

5 Simulations of solar cell

5.1 I-V Characteristics and Fill Factor

Using the above model, the solar cell was simulated and the dependence of the output current on various circuit elements in the model is observed. For all the simulations, the following typical values are assumed: $R_{sh} = R_{ext} = 1k\Omega cm^2$; $C_{trap} = 2nF/cm^2$; $C_{fast} = 20nF/cm^2$. The value of R_s depends upon the setup of the cell and the quality of electrical contact. Value of series resistance can vary in a very wide range from less than $1\Omega cm^2$to a few $k\Omega cm^2$. For simulations the value $R_s = 100\Omega cm^2$ has been chosen. The value of source I_p is set such that V_{OC} lies in its typical range of $550mV$ to $750mV$. The value of $I_p$used in this case is $4mA/cm^2$.

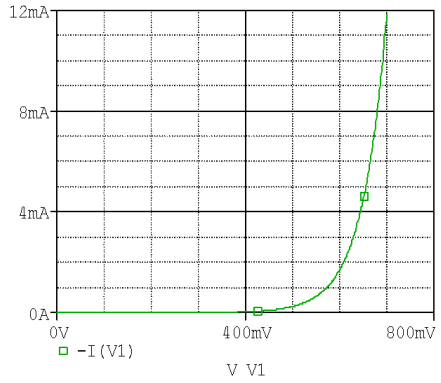

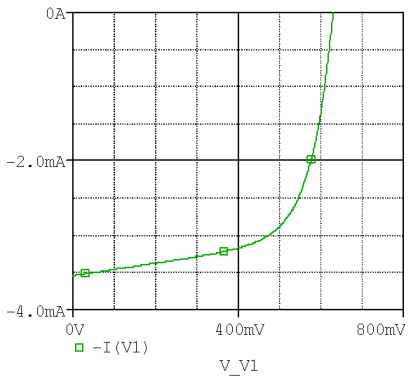

As was stated earlier and can be seen in the I-V curve above, current output goes on decreasing as the voltage is increased. Hence there is a particular value of voltage V_p, at which the cell delivers maximum power output. This point is called as peak power point (PPP). Fill factor is defined as the ratio of power delivered by the cell at PPP to the total area under the I-V curve in the IV quadrant. In the figure shown below, $V_p = 450mV$ and fill factor is roughly equal to 0.66.

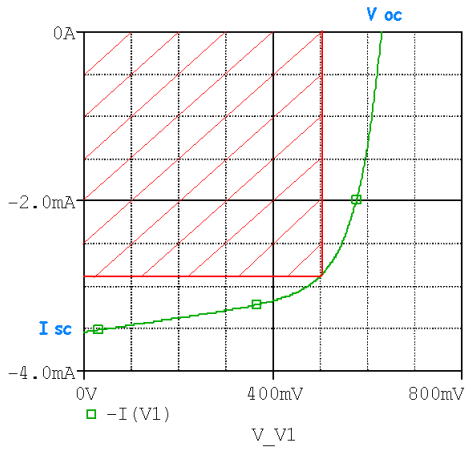

The images show the I-V characteristics of the solar cell in light and dark. In the light conditions, $V_{OC} \approx 630mV$ and $I_{SC} \approx 3mA/cm^2$.

The following four graphs show how the I-V characteristics of the cell forR_s equal to 125, 100, 75 and 50 Ohm-sqcm. respectively keeping all other parameters constant.

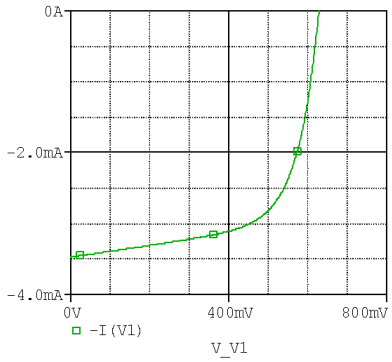

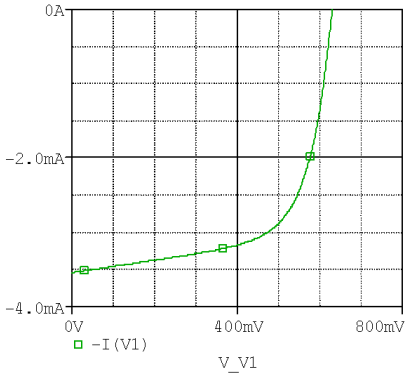

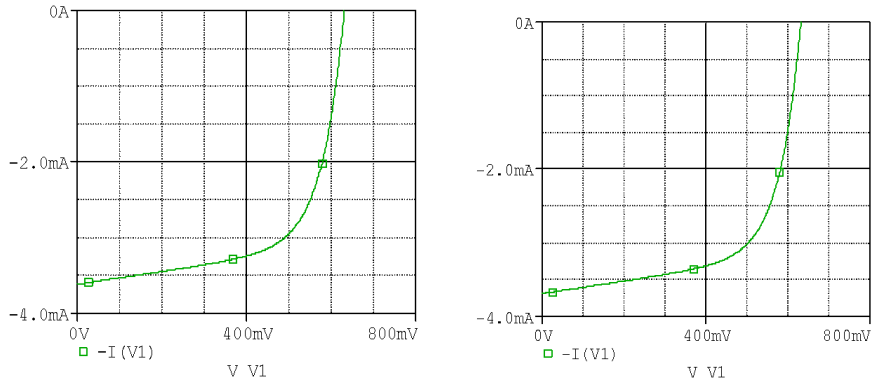

From the graph, we can conclude that for the same value of V_{OC}, I_{SC} is larger for smaller value of R_s. Thus, a solar cell with smaller $R_s$is preferable.

Similarly, the I-V characteristics are compared for R_{sh} values 0.5, 1, 3, $5k\Omega cm^2$ respectively.

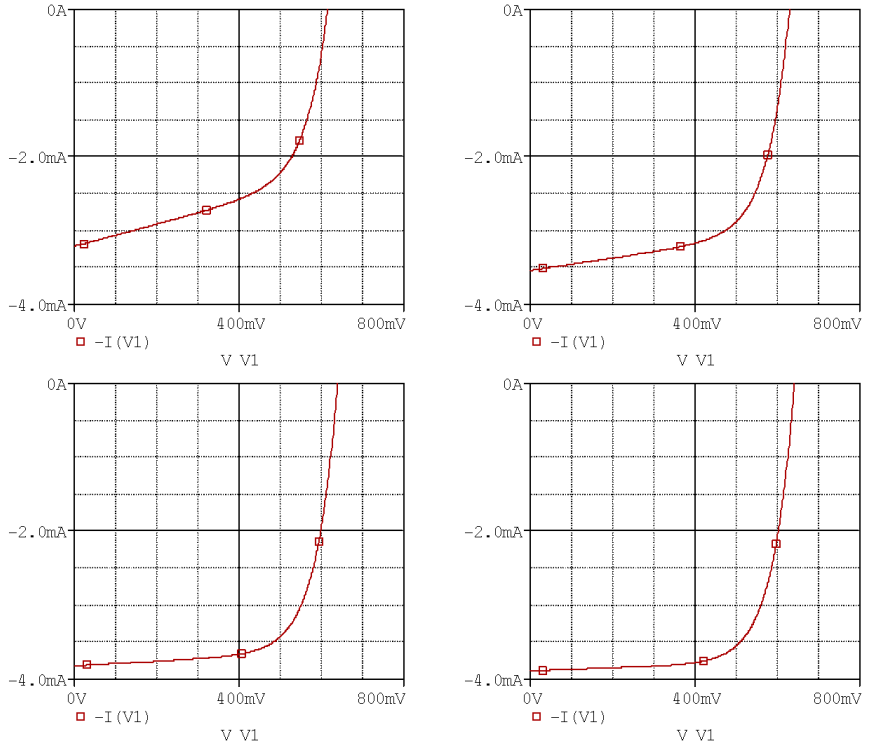

From the graphs one can observe that the fill factor of the I-V curve improves is R_{sh} increases. In the above case, fill factor increased from 0.56 to 0.62 for R_{sh} equal to 0.5 and $5\Omega cm^2$ respectively. This is because, smaller the value of R_{sh}, larger are the internal losses in the cell, I_p being constant. Hence, cells with larger value of R_{sh} are prefered.

5.2 AC Sweep

The DC sweep or the I-V plot only gives us information about the resistance parameters in the cell. However, to get information about the knee frequency (KF) and how it varies with different parameters, AC sweep is mandatory. AC sweep is used for impedance measerement of the solar cell. For AC sweep, I_p is an AC source and its frequency is sweeped from $10Hz$ to $100kHz$ and amplitude of the output current is plotted versus frequency. In the following simulations, an effort has been made to show how the frequency characteristics change with changes in different paramerters. Note that in most of the graphs, frequency is plotted in logarithmic scale.

Knee Frequency (KF): KF is the frequency above which the current amplitude shows a sudden drop. Thus, knee frequency is the maximum frequency upto which the cell is responsive. The time corresponding to KF is called the Response Time (RT) of the cell. RT gives the time resolution of the cell. For example, if amplitude of the light incident on the cell varies faster than the RT of the cell, then the cell will not be able to "see" the variations. Thus, when the cell is being used as a photodetector, larger KF is prefered.
Following plots show the frequency characteristics for R_{sh} equal to 10, 5, 1 and 0.3 $k\Omega cm^2$ respectively.

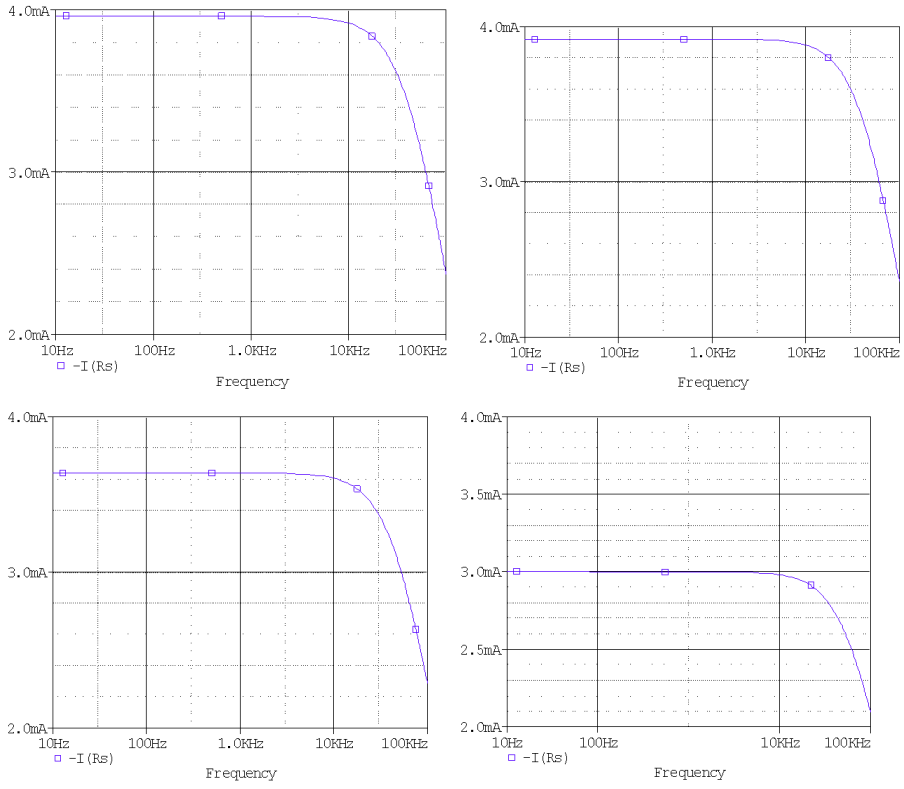

Observations There is a knee at around $15kHz$. The overall amplitude goes on falling with decrease in R_{sh}.
Following graphs show variation of frequency characteristics when R_s varies as 1000, 500, 100, 10 Ωcm^2.

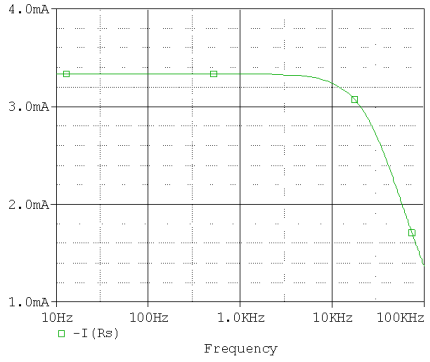

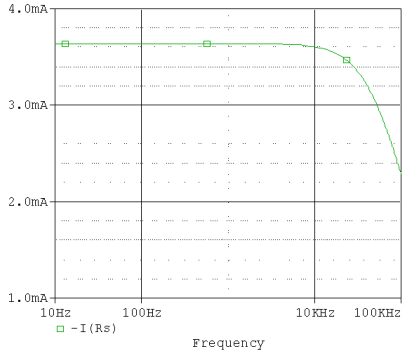

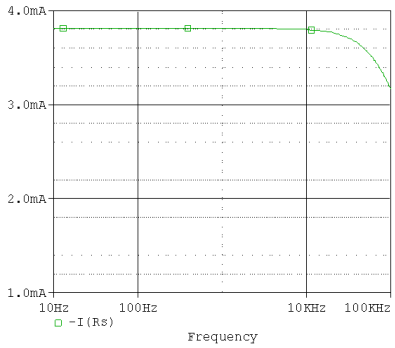

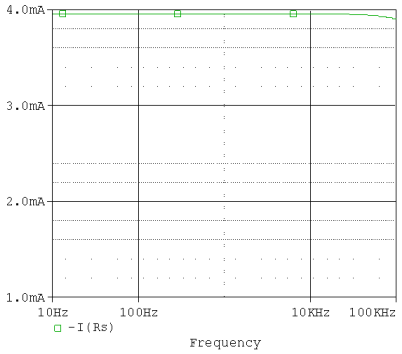

As R_s decreases, the knee frequency and the overall amplitude of the current increases.
Following frequency characteristics are ploted for C_{fast} equal to 200, 100, 50, 1 nF/cm^2.

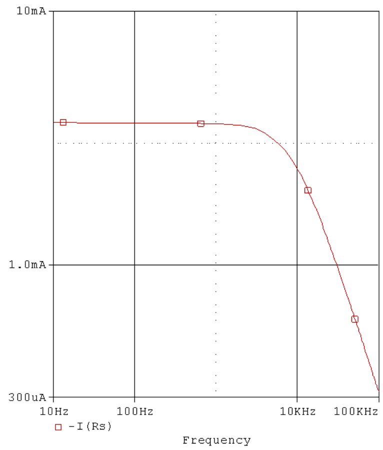

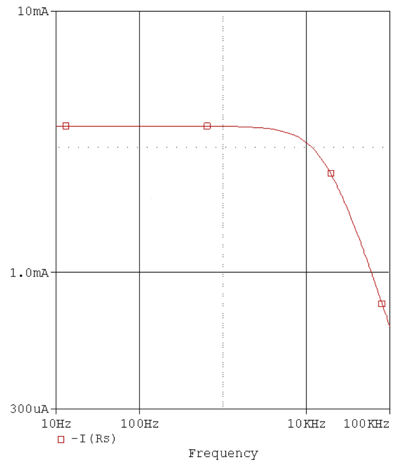

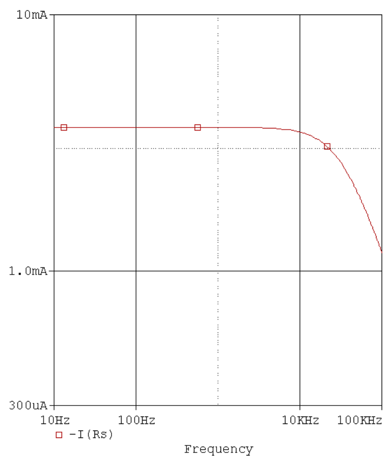

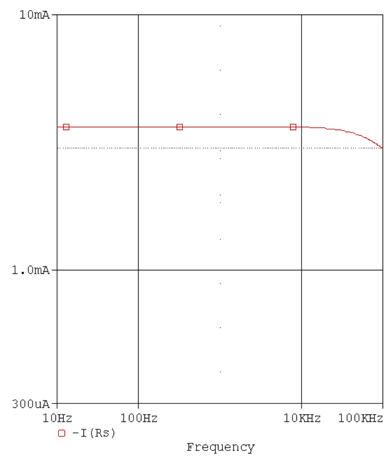

Knee frequency increases rapidly with drcrease in value of C_{fast}. Following function characteristics are for C_{trap} equal to 20, 10, 1, 0.1

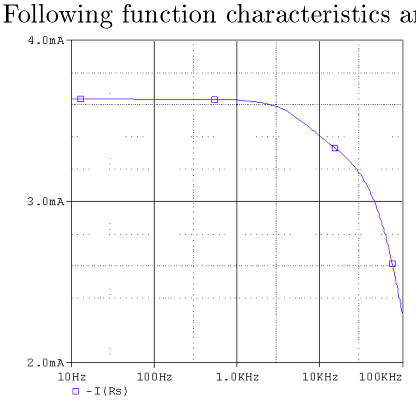

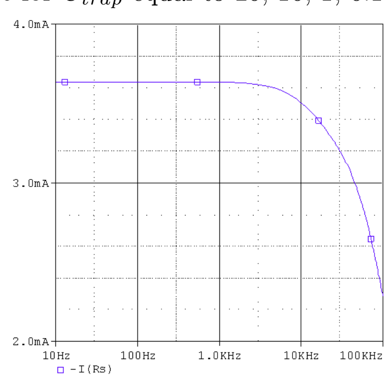

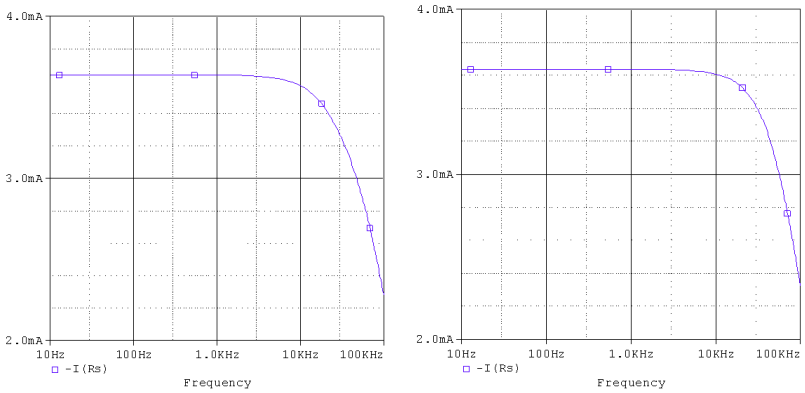

Following frequency characteristics are plotted for C_s equal to 10, 50, 100, 200 nF/cm^2.*

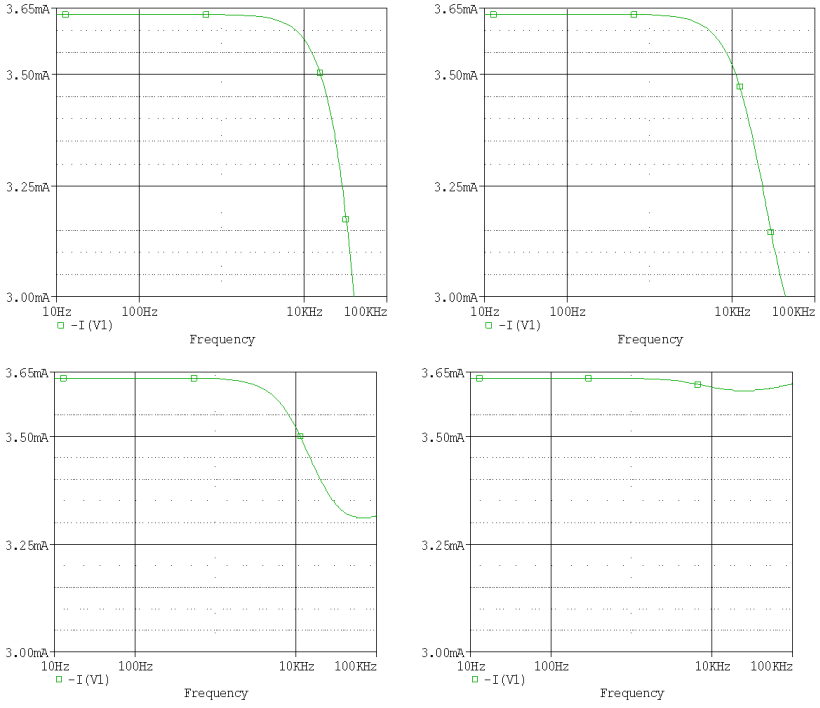

The common feature seen in all of these graphs is a knee frequency at around $10kHz$ and then a steep fall in current. Before the knee frequency, current output is quite high and nearly constant. However, experimentally obtained frequency sweep curves show a different feature. Experimentally obtained curves show a nearly constant current and then a sharp maximum at roughly 5-$10kHz$ and then a steep fall. This difference can be attributed to the polaron generation current itself to be frequency dependent. This is because the polaron generation involves many internal processes. The basic prevailing microscopic

kinetic processes of carrier generation, recombination and charge carrier trapping along with associated rate constants form the microscopic $I_p(\omega)$ as shown in the figure.

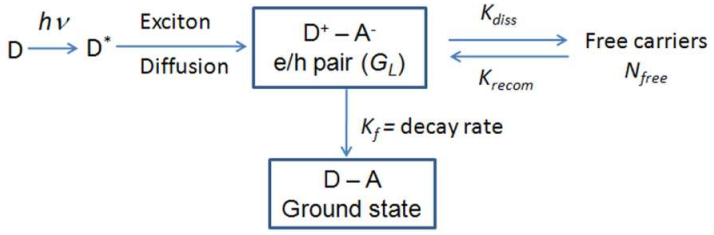

The microscopic processes span over multiple time scales (ps – ms). The associated parameters are: primary excitons generation rate (g_L), exciton diffusion lifetime ($\tau_1 \sim ns$), charge-carrier (n_{free}) life time τ_2, secondary exciton generation process and trapping kinetics. All of these processes depend on frequency causing polaron generation current to depend on frequency. To account for this the model should not only include the circuit of resistors and capacitances as given in section 4.4, but also that the resistors and capacitors should themselves be functions of frequency.

6 Extracting Physical Parameters from Given I-V Curve*

6.1 Extracting R_s and R_{sh} using slopes

From the circuit model, one can easily see that the effect of R_s becomes negligible at voltages close to V_{oc}. Hence the slope of the I-V curve at $V = V_{oc}$, is equal to $1/R_{sh}$. Also, under short circuit conditions, R_s and R_{sh} are in parallel. Therefore slope of the I-V curve at $V = 0$ is equal to $R_s^{-1} + R_{sh}^{-1}$. However, since $R_s \ll R_{sh}$, the $1/R_{sh}$ term may be neglected. Thus, slope of I-V curve at $V = 0$ is approximately equal to $1/R_s$. However, this method has a disadvantage that it may be very difficult to measure the slopes of the I-V curve accurately at the short circuit and open circuit ends [7-9].

6.2 Extracting Parameters Using the Four Point Method

The five cell parameters are

- Dark Current Density (J_o) at V_{oc}
- Photogenerated Current Density (J_{ph})
- R_s
- R_{sh}

- Diode Ideality Factor (η)

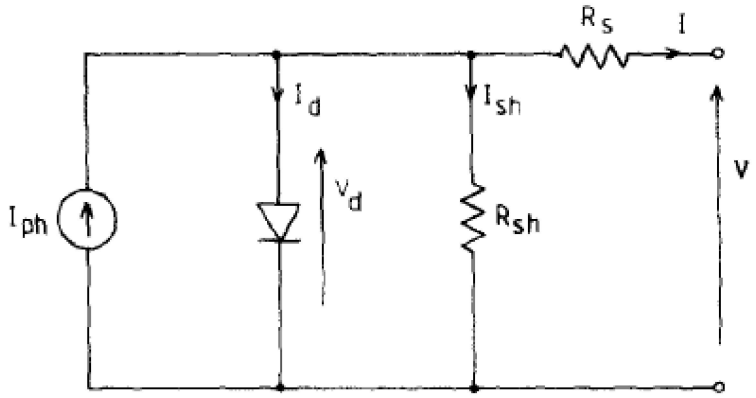

This method is a simple explicit power-law J–V model that is applicable to a wide variety of solar cells. This method allows an easy prediction of the entire J–V curve, peak power point, and fill factor (assuming single diode model of solar cell shown above) from four simple measurements of the bias points corresponding to Voc, 0.6 Voc, Jsc, and 0.6 Jsc, where Voc is the open-circuit voltage and Jsc is the short-circuit current density. Four points are needed on the I-V curve. Note that the measurement points should not be close to either the short- or open-circuit point because small measured values are prone to large percentage errors. On the other hand, a point on the sharply turning curve corner also gives erroneous results because the neglect of the term v_m in the derivation of γ is invalid for this condition. This is the reason for choice of 0.6 [7].The I-V curve of a solar cell by nature of an implicit form and hence is difficult to deal with.
In this method, the I-V curve is fitted with an explicit power law model which works for a wide range of cells. For this purpose we denote J/J_{sc} by j and V/V_{oc} by v. Then the I-V curve can be expressed as [8]

$$j = 1 - (1 - \gamma)v - \gamma v^m \tag{9}$$

When v is small, the linear term dominates fitting the slow fall in current near the short circuit end while the power law term models the steep fall near V_{oc}. Let the current density and voltage at the peak power point be denoted by v_p and j_p respectively. Then we have the relation

$$\frac{\delta(jv)}{\delta v} \mid_{v=v_p} = 0 \tag{10}$$

Solving this we get

$$1 - 2(1 - \gamma)v_p - \gamma(m + 1)v_p^m = 0 \tag{11}$$

and for $\gamma = 1$, it turns into $v_p = (1+m)^{-1/m}$. Then the above equation is empirically adjusted [7] as

$$v_p \approx (m+1) - 1/m - 0.05(1-\gamma) \tag{12}$$

Thus, v_p is obtained and hence j_p and FF can be found out.
Now we find out m and γ in terms of current density and voltage at the four points of measurement. m usually ranges from 7 to 15 while γ lies between 0.9 and 1.0.

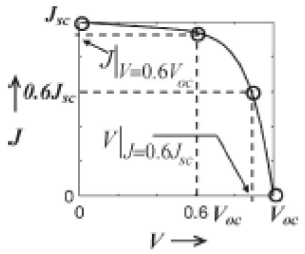

At $v = 0.6$, $v^m \ll 1$ and hence can be ignored. Therefore, at $v = 0.6$, eqn 9 gives us

$$(1-\gamma) \times 0.6 = 1 - j\mid_{v=0.6} \tag{13}$$

Thus

$$\gamma = \frac{j\mid_{v=0.6} - 0.4}{0.6} \tag{14}$$

Knowing γ, m can be found out easily as

$$m = log\left(\frac{0.4 - (1-\gamma)v\mid_{j=0.6}}{\gamma}\right) / logv\mid_{j=0.6} \tag{15}$$

The single exponential current density-voltage equation of an illuminated solar cell is given by [8-9]

$$J = J_{ph} - J_o(e^{\frac{V+JR_s}{\eta V_t}} - 1) - \frac{V + JR_s}{R_{sh}} \tag{16}$$

where, V_t is the thermal voltage of diode[4]. From the model, we can get the following equations

$$I_s(e^{\frac{V_{oc}}{nV_t}} - e^{\frac{I_{sc}R_s}{nV_t}}) - I_{sc}(1 + \frac{R_s}{R_{sh}}) + \frac{V_{oc}}{R_{sh}} = 0 \tag{17}$$

$$(R_{so} - R_s)(\frac{1}{R_{sh}} + \frac{I_s}{nV_t}e^{\frac{V_{oc}}{nV_t}}) - 1 = 0 \tag{18}$$

[4]Thermal Voltage at any temperature T is given as $V_t = kT/q$, where k is the Boltzmann constant and q is the electronic charge.

$$\frac{1}{R_{sh}} - \frac{1}{R_{sho} - R_s} + \frac{I_s}{nV_t} e^{\frac{I_{sc}R_s}{nV_t}} = 0 \tag{19}$$

$$I_s e^{\frac{V_{oc}}{nV_t}} + \frac{V_{oc} - V_p}{R_{sh}} - (1 + \frac{R_s}{R_{sh}})I_p - I_s e^{\frac{V_p + R_s I_p}{nV_t}} = 0 \tag{20}$$

where, I_p and V_p are current and voltage at peak power point, R_{so} and R_{sho} are reciprocals of slopes of the I-V curve at open circuit and short circuit points respectively, and n is the diode ideality factor. The above four equations can be simplified taking into account typical values of various parameters leading to four equations below

$$I_s e^{\frac{V_{oc}}{nV_t}} - I_{sc} + \frac{V_{oc}}{R_{sh}} \tag{21}$$

$$(R_{so} - R_s)\frac{I_s}{nV_t} e^{\frac{V_{oc}}{nV_t}} - 1 = 0 \tag{22}$$

$$R_{sh} = R_{sho} \tag{23}$$

$$I_s e^{\frac{V_{oc}}{nV_t}} + \frac{V_{oc} - V_p}{R_{sh}} - I_p - I_s e^{\frac{V_p + R_s I_p}{nV_t}} = 0 \tag{24}$$

Solving these equations expressions for R_s, I_s, I_{ph} and n can be obtained.

$$n = \frac{V_p + R_{so}I_p - V_{oc}}{V_T\left(ln(I_{sc} - \frac{V_p}{R_{sho}} - I_p) - ln(I_{sc} - \frac{V_{oc}}{R_{sh}}) + \frac{I_p}{I_{sc} - (V_{oc}/R_{sho})}\right)} \tag{25}$$

$$I_s = (I_{sc} - \frac{V_{oc}}{R_{sh}})e^{\frac{-V_{oc}}{nV_t}} \tag{26}$$

$$R_s = R_{so} - \frac{nV_t}{I_s} e^{\frac{-V_{oc}}{nV_t}} \tag{27}$$

$$I_{ph} = I_{sc}(1 + \frac{R_s}{R_{sh}}) + I_s(e^{\frac{I_{sc}R_s}{nV_t}} - 1) \tag{28}$$

Starting with the above equations, we express R_{sho} and R_{so} as

$$R_{so} = \frac{V_{oc}}{J_{sc}} \times \frac{1}{\gamma(m-1)+1} \tag{29}$$

$$R_{sho} = \frac{V_{oc}}{J_{sc}} \times \frac{1}{(1-\gamma)} \tag{30}$$

Hence n after some very simple algebraic manupulations can be written as

$$n = \frac{V_{oc}(v_p + \frac{j_p}{\gamma(m-1)+1} - 1)}{V_T\left(mlnv_p + j_p/\gamma\right)} \tag{31}$$

Thus, n can be computed since we already know V_{oc}, v_p, j_p, m and γ. Similarly substituting for R_{so} and I_s , we can express R_s as

$$R_s = \frac{V_{oc}}{J_{sc}\gamma} \times \left(\frac{1}{(m-1)+1/\gamma} - \frac{nV_t}{V_{oc}} \right) \tag{32}$$

R_s, R_{sh} and n have been extracted. Now we proceed towards extraction of J_o and J_{ph}. Equation (16) when evaluated at open and short circuit points lead to the following two equations.

$$0 = J_{ph} - J_o(e^{\frac{V_{oc}}{\eta V_t}} - 1) - \frac{V_{oc}}{R_{sh}} \tag{33}$$

$$J_{sc} = J_{ph} - J_o(e^{\frac{J_{sc}R_s}{\eta V_t}} - 1) - \frac{J_{sc}R_s}{R_{sh}} \tag{34}$$

Solving them simultaneously, J_o and J_{ph} can be found.

$$J_{sc} = J_o(e^{\frac{V_{oc}}{\eta V_t}} - e^{\frac{J_{sc}R_s}{\eta V_t}}) - \frac{V_{oc} - J_{sc}R_s}{R_{sh}} \tag{35}$$

Assuming that $J_{sc}R_s \ll V_{oc}$, the equation can be further simplified as

$$J_o = \gamma J_{sc} e^{\frac{-V_{oc}}{\eta V_t}} \tag{36}$$

Similarly, using above three equations, J_{ph} is extracted.
The parameter ξ introduced in section 4 can also be found out using J_o.

$$\xi = \gamma e^{\frac{-V_{oc}}{\eta V_t}} \tag{37}$$

7 Electrolyte Polymer Interface(EPI)

7.1 Basic Theory

Let us consider the interface betwen electrolyte solution and a semicinductor electrode. For the two phases are in equilibrium, they should have the same chemical potential. The potential of the electrolyte solution is determined by the redox potential of the solution. The chemical potential of the emiconductor electrode is determined by the Fermi Level (FL)[5]. For an n type semiconductor, FL is usually higher than the redox potential and hence electrons flow from the semiconductor to the electrolyte to balance the charges. Thus, the semiconductor gets a net positive charge which does not remain confined to the boundary (like it would if we had metal instead of semiconductor) but diffuses into the body of the semiconductor. The magnitude of charge in the semiconductor

[5]Fermi Level (FL) is defined as the energy level at which the probability of occupation of the level by an electron is exactly half. For a pure intrinsic semiconductor without doping, FL lies at the midpoint of the Band Gap. For a p-tye semiconductor, FL lies just above the valence band whereas for an n-type semiconductor, it lies just below the conduction band.

varies decreases exponentially with distance from EPI. Similarly, a p-type semiconductor would aquire a net negative charge. This charged region inside the semiconductor is called Depletion Region since the majority charge carriers are depleted in this region. This region is also called as Space Charge Region (SCR) and its thickness usually ranges from $10nm$ to $1\mu m$ [10]. This accumulation of charge leads to ban bending (Refer figure). (E_F, E_C and E_V stand for energies of FL, conduction band and valance band respectively.)

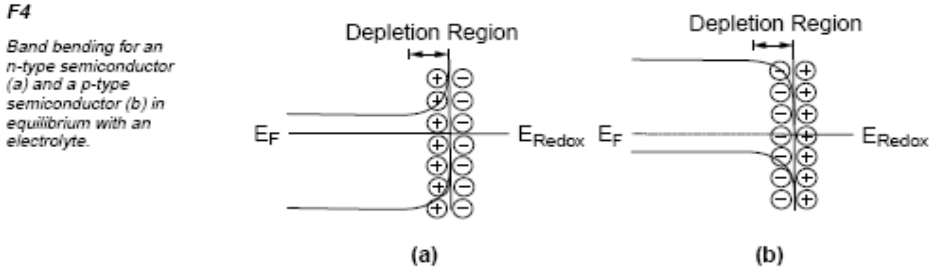

When an external potential is applied to the semiconductor, its band shift in accordance with the applied potential for the interior of the conductor. The bands at EPI however do not change because there is charges flow from electrolyte to semiconductor or vice-versa so that potential of both the phases is equal at EPI. Thus, depletion regions arise at potentials positive of the flatband potential for an n-type semiconductor and at potentials negative of the flatband potential for a p-type semiconductor. Under opposite conditions, accumulation regions (i. e. majority charge carriers increase in this region) will arise.
The charge transfer abilities of a semiconductor electrode depend on whether there is an accumulation layer or a depletion layer. If there is an accumulation layer, the behavior of a semiconductor electrode is similar to that of a metallic electrode, since there is an excess of the majority of charge carrier available for charge transfer. In contrast, if there is a depletion layer, then there are few charge carriers available for charge transfer, and electron transfer reactions occur slowly, if at all.
EPI is also used in solar cells. When light falls on the semiconductor, electrons are promoted to the conduction band. In the interior of the semiconductor, recombination of promoted electrons and the resulting holes takes place leading to heating of the cell. However, if the electron promotion occurs in the SCR, the electric field present in SCR forces the electron and hole to move away from eachother. This leads to output current. Thus, the thickness of the semiconductor electrode should ideally be equal to the thickness of SCR so that all of the incident light will be converted to output current. Practically however, the minimum thickness of the photoelectrode necessary for efficient light absorption is considerably more than the thickness of SCR. This is the cause of low efficiency of solar cells. (For details about solar cells, refer sections 4 and 5).
N-type semiconducting electrode at positive potentials (with respect to FB) and

p-type electrode at negative potentials (with respect to FB) act as photoanodes and the corresponding electrolyte soltions act as cathodes.

7.2 Model for EPI

On, one side there is semiconductor equivalent circuit and on the other side is the electrolyte equivalent circuit. The two circuits are connected by a capacitance. The equivalent circuit for EPI is shown below.

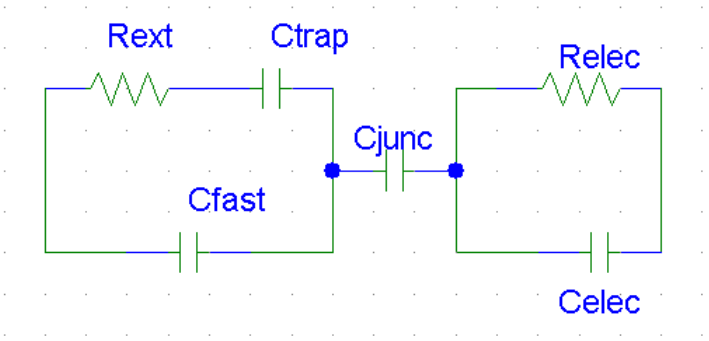

The junction capacitance arises due to the Space Charge in the semiconductor and the charge accumulation at the EPI.

8 Study of Electronics of Nerves

8.1 Generation of Nerve Impulse

8.1.1 Resting Neuron

Within the nervous system, signals travel yo and fro from brain to various parts of the body in the form of electrical impulses. When the nerve is not sending impulses, it is said to be 'resting'. The potential within the cell membrane during the resting period is called Resting Potential (RP), which is usually negative, due to negatively charged proteins inside the cell and a higher concentration of K^+ions outside. Typical value of RP is $\sim -70mV$ in humans. Also, the concentration of K^+ions is typically more outside the cell than inside while that of Na^+ions is more inside the cell than outside. This constant gradient is maintained by Sodium-Potassium Pumps (SPP) which pumps ions in suitable directions to maintain this gradient.

8.1.2 Action Potential

In addition to the SPP, there also exist voltage gated channels (VGC) for transport of sodium and potassium ions. These gates open on close depending upon

the potential difference across the membrane. If a neuron is stimulated beyond the threshhold potential (typically $-30mV$ in humans), the sodium channels open and sodium rushes into the axon, causing a region of positive charge within the axon. This process is called Depolarization of the axon. This brief reversal of the axon potential is called Action Potential. Due to accumulation of positive charge inside the axon, the sodium channels quickly close and the potassium channels open letting potassium ions out to restore the cell potential. All of this happens roughly $2ms$. The SPP again pumps ions to restore the ion gradient. This process continues like a chain reaction down the axon. Thus the nerve impulse propagates along the axon.

8.2 Neuron Equivalent Circuit

VGC are electrically represented by a DC power supply in series with a variable resistor which varies with voltage across the membrane as well as time. The equivalent circuit consists of two such VGC - one for sodium and other for potassium in parallel as shown in the circuit diagram.

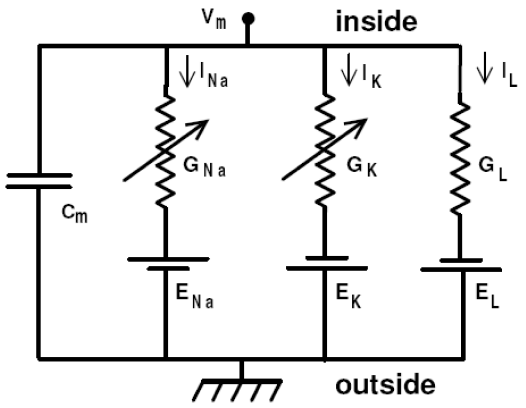

V_{in} respresents the inside potential of the cell. Because the charge concentration inside and outside the cell is not equal, a membrane capacitance needs to be added along with two VGC. Also even when the channels are closed, there exists a small leakage current represented by a DC voltage source and a constant resistance.

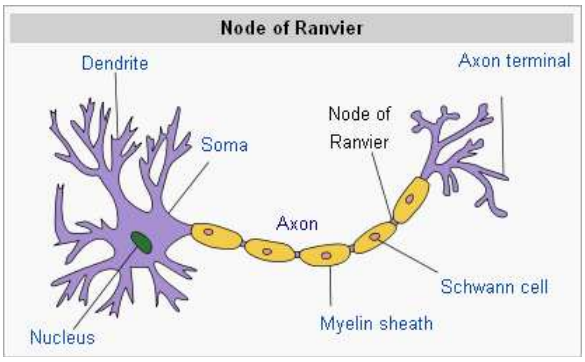

The nerve cell or the axon consists of myelin sheaths generated by different cells separated by Nodes of Ranvier. The portion of axon between two such nodes is called a compartment. So, an axon consists of many compartments. joined together by Nodes of Ranvier. The circuit above represents one compartment. The equivalent circuit of an entire axon is got by joining together a number of above circuits each separated by a resistance. The way in which these electrical units are joined together dependes upon the shape of the axon and its extent of branching.

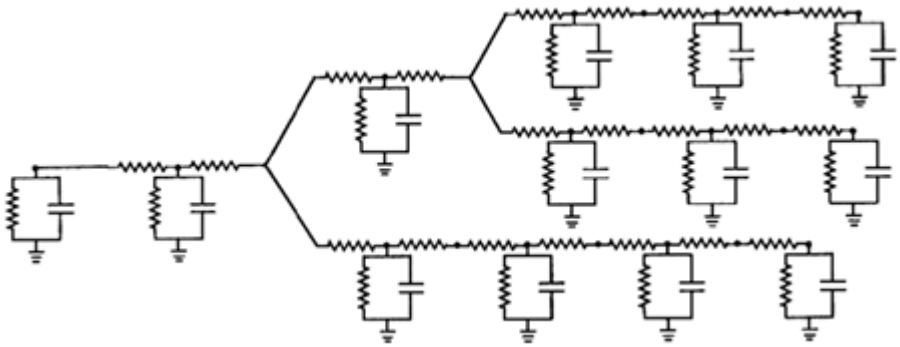

The nerves in the human retina show a peculiar response. They give out a burst of spikes superimposed over the main spike as shown in the figure. The figure below shows the response obtained by simulation of the equivalent circuit for retinal neurons.

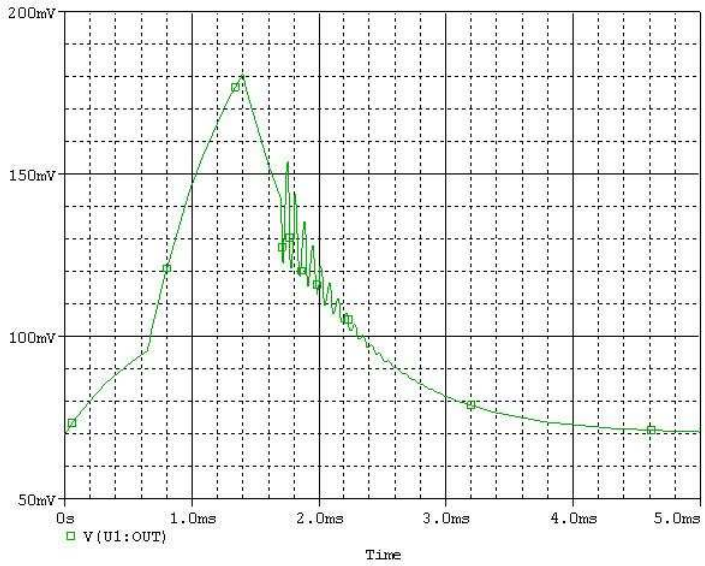

The equivalent circuit of these nerves can be generated by superimposing a separately generated spike-train of exponentially decaying amplitude over the main peak using an adder circuit. One of the possible equivalent circuits is shown below.

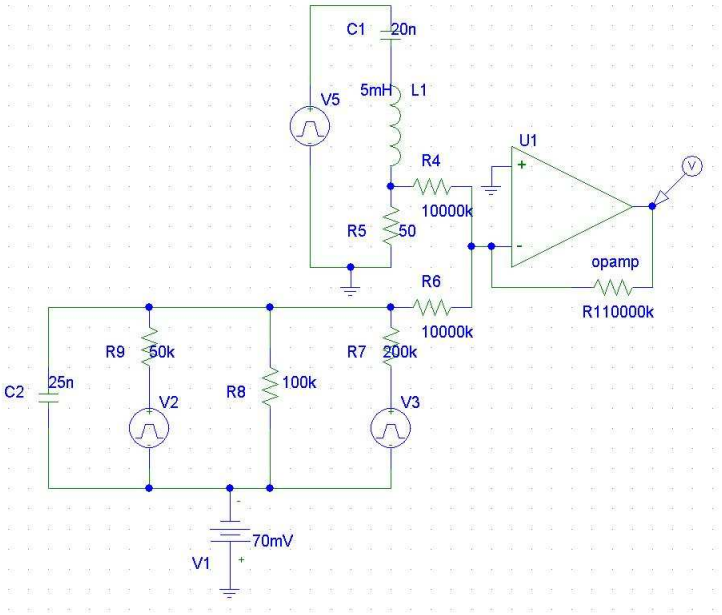

The amplitude, rate of amplitude decay etc. can be controlled using the RLC values while the shape of the main peak is controlled by the neuron equivalent circuit as before.

9 Acknowledgements

My sincere thanks to JNCASR for giving such a wonderful opportunity to students. I am deeply indebted to Prof. K. S. Narayan for his invaluable support and guidane. I am equally indebted to Prof. Vidhyadhiraja[6] for his time and guidance. I also thank Monojit Bag[7] for his help.

References

[1] Juan Bisquert, Physical Review B 77, 235203 (2008).

[2] Juan Bisquert, Electrochimica Acta 47 (2002) 2435/2449.

[3] C.-T. Sah, Fundamentals of Solid State Electronics World Scientific, Singapore, 1991

[4] S. Uchida, J. Xue, B.P. Rand, S.R. Forrest, Appl. Phys. Lett. 84 (2004) 4218.

[5] B. Mazhari, Solar Energy Materials & Solar Cells 90 (2006) 1021–1033.

[6] IV and CV Characterizations of Solar/ Photovoltaic Cells Using the B1500A, Application Note B1500A-14.

[7] Shreepad Karmalkar and Saleem Haneefa, IEEE Electron Device Letters, Vol. 29, No. 5, May 2008.

[8] H. Saleem and Shreepad Karmalkar, IEEE Electron Device Letters, Vol. 30, No. 4, April 2009.

[9] D. S. H. Chan, J. R. Phillips and J. C. H. Phang, Solid-State Electromcs Vol. 29, No. 3. pp. 329-337, 1986

[10] Electrochemistry of Semiconductors, Adrian W. Bott, Ph.D. Bioanalytical Systems, Inc. 2701 Kent Avenue West Lafayette, IN 47906-1382.

[11] http://www.biologymad.com/NervousSystem/nerveimpulses.htm

[12] http://www.biology4all.com/resources_library/source/63.swf

[13] http://www.brains-minds-media.org/archive/218

[14] http://en.wikipedia.org/wiki/Node_of_Ranvier

[6] Theorotical Science Unit, JNCASR

[7] Ph. D. student, Molecular Electronics Lab, JNCASR